FLOW IN THE ANNULUS OF A WATER SPOUTED BED OF SMALL GLASS PARTICLES AT MINIMUM SPOUTING

SEUNG JAI KIM AND JOON HO HA
Department of Chemical Engineering, Chonnam National University, Kwangju, Chonnam 505, Korea

Key Words: Minimum Spouting, Cylindrical Half Column, Small Particles, Water, Darcy Flow, Axisymmetric Model, Residence Time

The flow in the annulus of a water spouted bed of small glass particles 0.574 mm and 0.964 mm in diameter is studied in a cylindrical half-column 90 mm in diameter.

An axisymmetric model of flow, which assumes Darcy flow in the annulus and uses the experimental spout-annulus interfacial boundary condition, predicts the annulus fluid streamlines of fine particle beds well.

The model calculations show that the average fluid velocity at the top of the annulus decreases as particle size and bed height decrease and the fluid residence time distribution in the annulus is broad.

Particles are observed entering the spout primarily near the spout inlet in agreement with the predicted axial voidage profile in the spout.

Introduction

The spouted bed is commonly thought of as being useful only for processes involving coarse particles. It has been studied quite intensively, but not much information is available for a bed of fine particles of $d_p < 1$ mm. Small particle systems are of interest theoretically because the inertial force of the jet at minimum spouting is small relative to the bed pressure drop.

In applying spouted bed technology to fluid-particle reactions, it is necessary to have a model of flow in the annulus of a spouted bed from which the residence time of the fluid and the amount of the fluid flowing through the annulus at any bed level can be calculated. Since one-dimensional models[3,9] developed for predicting the axial pressure and velocity distributions of the fluid in the annulus of a spouted bed cannot predict the actual streamlines, they are not useful whenever such information is important.

There are two types of axisymmetric flow models in the literature. Lefroy and Davidson[5] solved a boundary value problem assuming Darcy flow in the annulus. This model has been modified by many workers.[2,7,16] The other type of axisymmetric flow model reported is that of Lim and Mathur.[6] The characteristics and differences of these models have been well described by Littman *et al.*[8]

Recently, Littman *et al.*[8] presented an axisymmetric flow model of the kind first proposed by Lefroy and Davidson[5] which took into account non-Darcy flow in the annulus. Using the Morgan and Littman[13] spout-annulus pressure boundary condition, they showed that the model represented the pressure and stream-function fields in the annulus well and calculated the axial velocity profile and the residence time distribution of the fluid.

In this work, the flow characteristics of a water spouted bed of small glass particles, 0.574 mm and 0.964 mm in diameter, are studied in a cylindrical half-column 90 mm in diameter. Using experimentally measured model parameters, an axisymmetric flow model of Lefroy and Davidson type[5] which assumes Darcy flow in the annulus is used to predict the streamline, velocity and residence time of the fluid there. The predicted streamlines and residence times of the fluid are compared with the experimental data. In addition, the axial fluid velocity and spout voidage profile are calculated and compared with those for air spouted beds of coarse particles.

1. Flow Model

For the spouting of small particles, $d_p < 1$ mm, with water, Darcy's law is applicable in the annulus at minimum spouting since the non-linear term in the Ergun equation is less than 10% of the linear term in general. The equations for the flow in the annulus are the same as those of Lefroy and Davidson[5] except for the spout-annulus interfacial boundary condition.

$$\nabla \cdot \bar{u} = 0 \tag{1}$$

$$\nabla P = -f_1 \bar{u} \tag{2}$$

The voidage in the spout is higher than that in the

Received October 30, 1985. Correspondence concerning this article should be addressed to S. J. Kim.

annulus and the bed voidage varies smoothly, axially as well as radially. However, we assumed that f_1 is constant since we observed that the voidage in the annulus was essentially constant except for the region very close to the spout-annulus interface.

From Eqs. (1) and (2), the pressure field in the annulus is

$$\nabla^2 p = 0 \tag{3}$$

For axisymmetric motion about the z axis of the cylinder, the boundary conditions are

$$\frac{\partial p(r,0)}{\partial z} = 0 \tag{4}$$

$$p(r, H) = 0 \tag{5}$$

$$\frac{\partial p(r_C, z)}{\partial r} = 0 \tag{6}$$

$$p(r_S, z) = f(z) \tag{7}$$

The spout-annulus interfacial boundary condition is obtained experimentally and described in terms of the polynomial

$$f(z) = p_{Si}(z) - p_{Si}(H) = \Delta P_{Si}(a + b\zeta + c\zeta^2 + d\zeta^3)$$

where a, b, c and d are constants. The values of these constants are given in Eqs. (9) and (10).

From Eqs. (2) and (3) together with the boundary conditions, we obtained the stream function in the annulus as

$$\psi(r,z) = -\frac{\Delta P_{Si}}{f_1} r \frac{I_1(mr)K_1(mr_C) - I_1(mr_C)K_1(mr)}{I_0(mr_S)K_1(mr_C) + I_1(mr_C)K_0(mr_S)} \times \sum_{n=1,3,5}^{\infty} \frac{C_n}{n} \sin(n\pi z/2H) \tag{8}$$

where

$$C_n = \left[-\frac{8b}{n^2\pi^2} - \frac{32}{n^3\pi^3}(c + 3d)\sin(n\pi/2) + \frac{192d}{n^4\pi^4} \right]$$

2. Experiments

The experiments were carried out in the apparatus shown schematically in **Fig. 1**. The spouted bed shown in the figure is a cylindrical half-column, 90 mm in diameter and 800 mm high. It is made of Plexiglas and has a flat base. The flat face of the half-column has a non-uniform rectangular grid of 44 pressure taps, all connected to the piezometer tubes. The water temperature was generally kept at about 25°C.

The bed pressure drop, annulus height, jet penetration and spout fountain height are shown in Fig. 2 as a function of flow rate for 0.964-mm particles. The bed is shallow enough for the jet to penetrate it. With increasing flow rate the jet begins to penetrate the bed, and as the flow rate is increased, penetration continues rapidly with decreasing bed pressure drop until

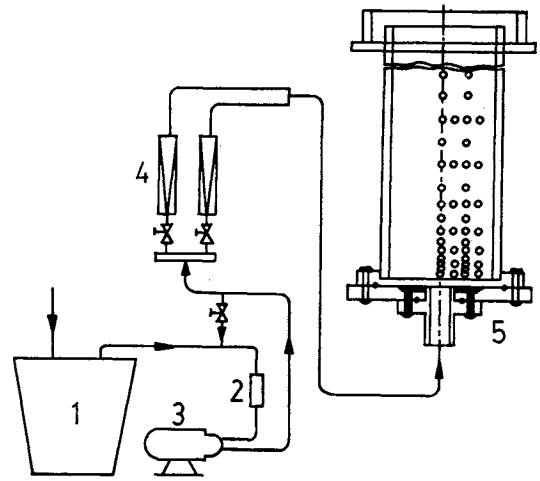

Fig. 1. Schematic diagram of experimental apparatus: 1, water tank; 2, water filter; 3, pump; 4, rotameter; 5, spouted bed. Arrows indicate direction of water flow.

the jet reaches the top of the bed at point A'. On decreasing the flow rate from above the minimum spouting, the jet ceases to penetrate the top of the bed at point A. This flow rate, seen in **Fig. 2**, is defined as the minimum spouting flow rate. ΔP_{mS} is the measured pressure drop, $[p_S(0) - p_S(H)]$, along the axis of symmetry in the minimum spouting condition. The spout-annulus interfacial pressure drop, ΔP_{Si}, is the pressure drop measured in the spout close to the interface and is essentially the same as ΔP_S.

Above a certain bed height, the jet does not penetrate to the top of the bed regardless of flow rate, because the bed expands faster than the jet can penetrate it. The criterion for determining H_m and $(u_{mS})_{H_m}$ for these beds was formulated by observing the change in shape of the jet with decreasing flow rate. As the fluid velocity is lowered from above $(u_{mS})_{H_m}$, the jet narrows at the top, finally assuming a flame tip shape. $(u_{mS})_{H_m}$ is the highest velocity for which the flame tip-shape jet is visible and is slightly higher than u_{mF} (**Tables 1** and **2**). The height of the spout to the tip of the flame shape jet at $(u_{mS})_{H_m}$ is denoted H_m. $(\Delta P_{mS})_{H_m}$ is the spout pressure drop at $(u_{mS})_{H_m}$ in the bed of height H_m.

The fluid streaklines and residence times were measured by use of dye tracer techniques. Methylene blue solution, 1% by weight, was injected into the annulus and the streakline was photographed and the residence time along the streamline measured. Using colored particles, the particle pathlines in the annulus along the flat face of the half-column were measured. During the experiment, no air bubbles were observed in the bed and the pressure readings were steady. A cylindrical column, 80 mm in diameter, was used to carry out the fluidization experiments.

The fluidization and particle properties of the system studied are listed in Table 1 and the spouted bed

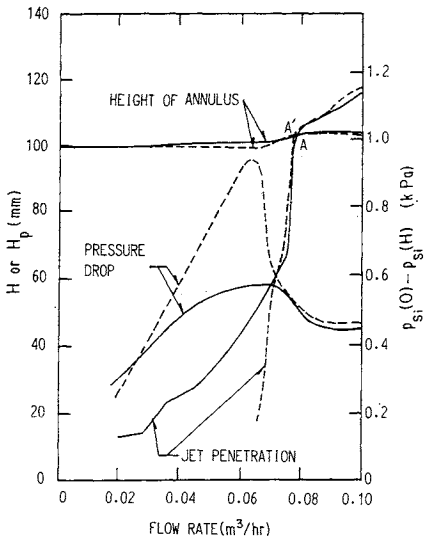

Fig. 2. Bed pressure drop, annulus height, jet penetration and spout fountain height as a function of flow rate: d_p = 0.964 mm; ----, increasing flow rate; ——, decreasing flow rate.

Table 1. Flow and particle properties of the system studied

$D_C = 80$ mm

d_p [mm]	ρ_p [kg/m^3]	υ [m^2/s]	ε_{mF}	u_{mF} [mm/s]
0.574	2340	0.894×10^{-4}	0.400	3.04
0.964	2460	0.894×10^{-4}	0.402	6.30

Table 2. Experimentally measured spouted bed properties

$D_C = 90$ mm, $D_h = 55$ mm, $d_i = 6.7$ mm

d_p [mm]	H [mm]	u_{mS} [mm/s]	d_S [mm]	ΔP_{mS} [kPa]	ΔP_{mF} [kPa]
0.574	40.0	1.31	9.0	0.200	0.318
	67.8	2.24	9.9	0.333	0.524
	88.0	2.68	10.6	0.445	0.683
	109.8	3.06	11.6	0.567	0.843
	130.8	3.36	12.8	0.716	1.006
	156.5*	3.46	13.8	0.918	1.207
0.964	67.0	5.03	12.3	0.331	0.541
	88.8	5.80	13.6	0.444	0.708
	103.2	6.74	14.6	0.515	0.820
	111.0*	6.81	15.1	0.558	0.877

* H_m.

properties in a bed of height equal to or less than H_m at minimum spouting are listed in Table 2. The particles are spherical and the average spout diameter listed in Table 2 is the mean value, that is, $\int_0^1 d_S(z/H)$.

3. Results and Discussion

3.1 Spout-annulus interfacial boundary condition

The spout-annulus interfacial boundary condition is the critical condition required for calculating the flow field in the annulus. For this reason, we measured the axial pressure in the spout close to the interface and compared it with the spout pressure distributions by various methods.[5,9,13]

As can be seen in Table 2, the normalized minimum spouting pressure drop, $\Delta P_{mS}/\Delta P_{mF}$, increases with H/H_m approximately linearly and reaches 0.760 and 0.636 at $H=H_m$ for 0.574 mm and 0.964 mm, respectively. These are in good agreement with the maxima predicted by the Mamuro and Hattori[9] and Lefroy and Davidson[5] theories (0.75 and 0.64, respectively). The Morgan and Littman[13] theory predicts that $(\Delta P_{mS})_{H_m}/\Delta P_{mF}$ decreases as the particle size is increased for a given system. However, their theory predicts the values for $(\Delta P_{mS})_{H_m}/\Delta P_{mF}$ as 0.502 for 0.574-mm and 0.402 for 0.964-mm particles, which are substantially lower values than those found experimentally.

The experimental pressure profile along the spout-annulus interface is normalized and correlated in terms of a third-degree polynomial. Our correlations for the normalized interfacial pressure profiles are

$$\frac{p_{Si}(z)-p_{Si}(H)}{\Delta P_{Si}} = 1.00 - 0.25\zeta - 1.11\zeta^2 + 0.36\zeta^3 \quad (9)$$

for 0.574-mm particles; correlation coefficient = 0.975 and

$$\frac{p_{Si}(z)-p_{Si}(H)}{\Delta P_{Si}} = 1.00 - 0.11\zeta - 1.16\zeta^2 + 0.27\zeta^3 \quad (10)$$

for 0.964-mm particles; correlation coefficient = 0.972.

Equations (9) and (10) are shown in **Fig. 3** along with the profiles of Grbavcic *et al.*[3] and Lefroy and Davidson.[5] The profiles of Morgan and Littman[13] fall in between those of Grbavcic *et al.*[3] and Lefroy and Davidson[5] and their theory predicts that the normalized pressure for 0.574-mm particles is slightly lower than that for 0.964-mm particles for a given value of z/H_m.

As can be seen in Fig. 3, the theories[3,5] represent the normalized interfacial pressure profile quite well. However, there are substantial differences between the experimental correlations and the theoretical profiles[3,5,13] in the slopes of the profiles as z/H_m approaches zero, which have again a substantial effect on the flow in the annulus and the spout voidage profile. Note that all the theories[3,5,13] predict that the slope of the normalized interfacial pressure profile at $z/H_m=0$ is zero, but our correlations give the values as -0.25 and -0.11 for 0.574-mm and 0.964-mm particles, respectively. For this reason, our correlations are used for model calculations. However, except for the region close to the spout inlet, the Grbavcic *et al.*[3] and Lefroy and Davidson[5] theories predict the spout pressure drops, $(\Delta P_{mS})_{H_m}/\Delta P_{mF}$, and

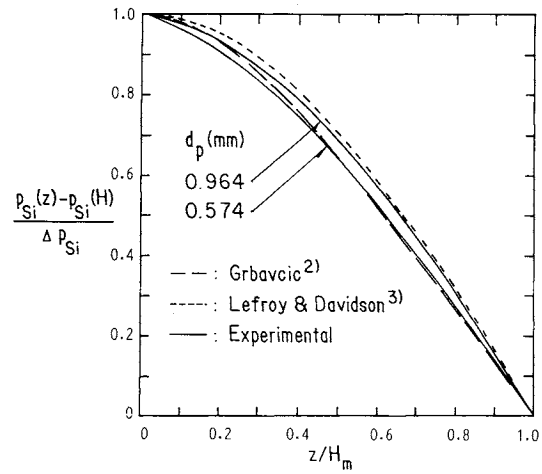

Fig. 3. Normalized spout-annulus interfacial pressure profile.

the normalized pressure profiles at the interface well overall for 0.574-mm and 0.964-mm particles, respectively.

3.2 Stream-function fields and streamlines

Equation (8) was used to calculate the fluid streamlines and velocities in the annulus, and the results are shown in **Figs. 4** and **5** for 0.574-mm and 0.964-mm particles, respectively, together with the measured fluid streaklines and particle pathlines. Each bed is at its maximum spoutable height in the condition of minimum spouting.

As can be seen in the figures, our model predicts the fluid streamlines well. It is generally known that the particle pathlines in the annulus of a gas spouted bed of coarse particles are approximately parabolic and practically identical with the fluid streamlines.[10)] In addition, the particle cross flow rate per unit height of the interface is constant.[10,11,17)]

For the spouting of small glass particles with water at minimum spouting, the particles are observed entering the spout primarily in the region close to the spout inlet, $z/H_m<0.3$, and reentering the annulus in the upper part of the bed, $z/H_m>0.7$, forming an inner circulation pattern as shown in Figs. 4 and 5. Grbavcic[4)] has reported the same particle circulation pattern in a water spouted bed of 2.5-mm glass particles at $u=u_{ms}$ and $H=H_m$ (see Figure S1.8 of Grbavcic). It is obvious that the particle cross flow rate from the annulus to the spout is not constant in this case. The particle velocity and circulation will be dealt with in another paper.

3.3 Average axial fluid velocity in the annulus

The radially averaged axial fluid velocity in the annulus was calculated from the model, and **Fig. 6** shows a comparison of the various models at the maximum spoutable height and in the condition of minimum spouting.

In the Lefroy and Davidson[5)] and Grbavcic *et al.*[3)]

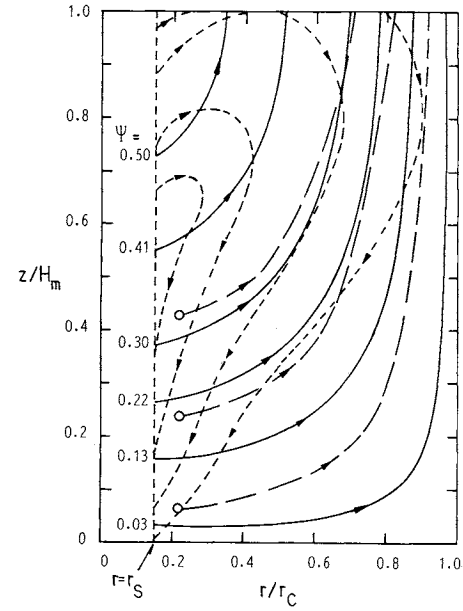

Fig. 4. Fluid streamlines and particle pathlines: $d_p=$ 0.574 mm; $u=u_{ms}$; $H=H_m$; ——, fluid streamlines (calculated); — —, fluid streaklines (measured); – – – –, particle pathlines (measured); ○, injection point of dye tracer.

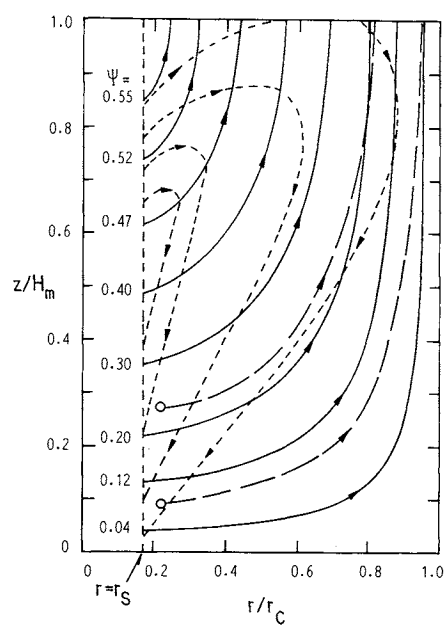

Fig. 5. Fluid streamlines and particle pathlines: $d_p=$ 0.964 mm; $u=u_{ms}$; $H=H_m$; ——, fluid streamlines (calculated); — —, fluid streaklines (measured); – – – –, particle pathlines (measured); ○, injection point of dye tracer.

models, $\langle u_a\rangle_{H_m}$ is equal to u_{mF} and $\langle u_a\rangle/u_{mF}$ is a unique function of z/H_m. Piccinini *et al.*[15)] modified the Grbavcic *et al.*[3)] model based on the experimental data of Epstein *et al.*[1)] and proposed

$$\frac{\langle u_a\rangle}{\langle u_a\rangle_{H_m}}=\frac{\langle u_a\rangle}{u_{mF}}=0.88\left[1-\left(1-\frac{z}{H_m}\right)^3\right] \qquad (11)$$

Recently, Littman *et al.*[8)] have shown from their axisymmetric flow model that $\langle u_a\rangle_{H_m}/u_{mF}$ is less than

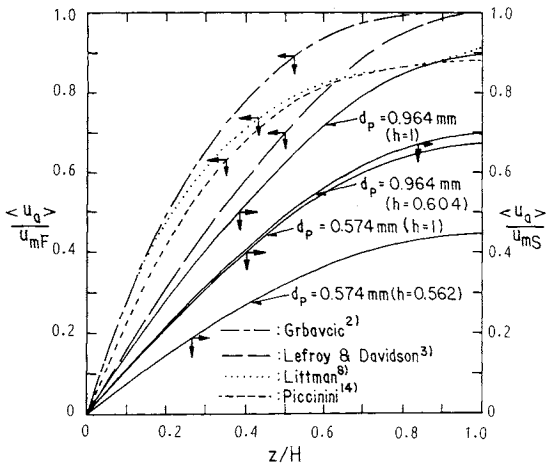

Fig. 6. Comparison of models predicting average axial fluid velocity in annulus: $u = u_{mS}$.

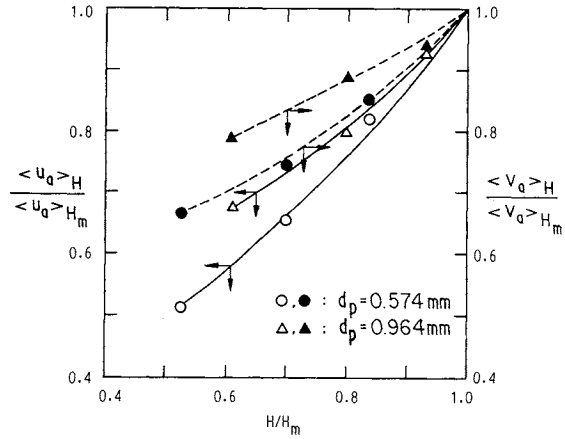

Fig. 7. Effect of bed height on average fluid velocity at top of annulus and portion of the fluid flowing through top of annulus: $u = u_{mS}$.

1 and Eq. (11) is in good agreement with their model predictions, even for beds of height less than H_m.

For coarse particle beds,[2,8] $(u_{mS})_{H_m}$ is equal to u_{mF}. In our experiments, $(u_{mS})_{H_m}$ is 13.8% above u_{mF} for 0.574-mm particles and 8.1% above for 0.964-mm particles (see Tables 1 and 2). For this reason, we normalized $\langle u_a \rangle$ with $(u_{mS})_{H_m}$ instead of u_{mF}.

As can be seen in Fig. 6, the model predicts that $\langle u_a \rangle / (u_{mS})_{H_m}$ increases with z/H_m and reaches 0.67 for 0.574-mm particles and 0.89 for 0.964-mm particles at $z/H_m = 1.0$. The value for 0.964-mm particles, 0.89, is similar to the coefficient in Eq. (11), 0.88, and the 0.925 figure given by Littman *et al.*[8] However, the value for 0.574-mm particles, 0.67, is substantially lower than those for coarse particles. In addition, the portion of the fluid flowing through the top of the annulus calculated at $u = u_{mS}$ and $H = H_m$, $[\langle u_a \rangle_{H_m}(D_C^2 - D_S^2)]/[(u_{mS})_{H_m} D_C^2]$, is 0.65 for 0.574-mm particles and 0.87 for 0.964-mm particles. Littman *et al.*[8] reported the portion to be 0.872 for 2.94-mm glass particles spouted with air. These show that both the fluid velocity and the portion of the fluid flow through the top of the annulus of a fine particle bed are substantially lower than those of coarse particle beds.

As the particle size is increased in the minimum spouting condition, the maximum spoutable height decreases but the spout diameter increases. These changes cause substantial increase in the spout-annulus interfacial area per unit volume of the annulus and the flow through the annulus as the particle size is increased.

As the bed height is reduced below the maximum spoutable height for each particle size, the model calculations show that both the average axial fluid velocity and the portion of fluid flowing through the top of the annulus decrease, as can be seen in **Fig. 7.**

3.4 Residence time distribution

The residence time of the fluid along the various streamlines was calculated from the model for a bed of height, H_m, at minimum spouting condition assuming the annulus voidage is ε_{mF}.

The calculated residence time distribution of the fluid in the annulus normalized by H_m/u_{mS} is shown in **Fig. 8** for 0.964-mm particles. The normalized residence time distribution for 0.574-mm particles was similar to that for 0.964-mm particles. As can be seen in Fig. 8, the fluid residence time distribution is broad and, as expected, the fluid entering the annulus near the spout inlet has a longer residence time than the fluid entering the annulus higher in the interface. This behavior is similar to that reported for coarse particle beds.[8]

To estimate the degree of deviation between measured and calculated residence time, the dye tracer was injected in the annulus at different locations and the results are shown in Fig. 8 for 0.964-mm particles for a bed at its maximum spoutable height in the condition of minimum spouting. Figure 8 shows that the calculated residence times are in all cases smaller than the measured ones with an average deviation of 27%, and that the deviations decrease slightly with closeness of the fluid streaklines to the column wall. Since we assumed smooth streaklines of fluid in the annulus (Figs. 4 and 5), the actual pathlines of the dye tracer would be longer than the ones we used in calculating the theoretical residence times in Fig. 8. This factor, which will reduce the deviation if taken into account, is under investigation.

3.5 Spout voidage and particle movement

The voidage distribution in the spout in low-inertia systems can be calculated from the simplified spout momentum equation. For the fluid and particle flow through an element of the spout assuming a constant spout diameter and radially averaged velocities,

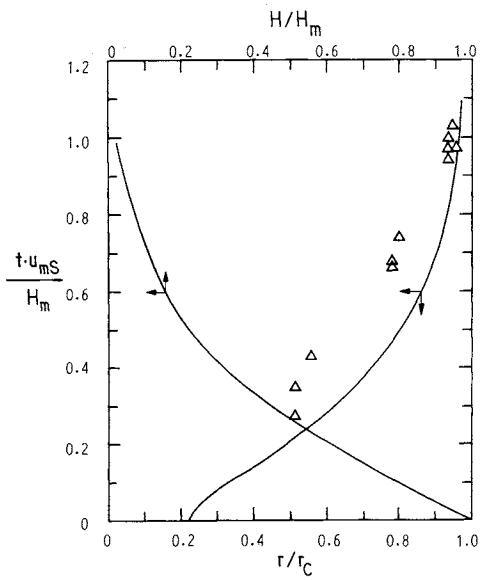

Fig. 8. Calculated residence time distribution as a function of distance from spout inlet at the interface and comparison of calculated and measured residence times of the fluid from injection point of dye tracer to top of annulus: $d_p = 0.964$ mm; $u = u_{mS}$; $H = H_m$.

$$\rho_f \frac{d}{dz}[\varepsilon_S u_S^2] + \rho_p \frac{d}{dz}[(1-\varepsilon_S)v_S^2] = -\frac{dp_S}{dz} - (1-\varepsilon_S)(\rho_p - \rho_f)g \tag{12}$$

Neglecting the inertial terms, which are small in our work at minimum spouting, we obtain

$$\varepsilon_S = 1 + \frac{1}{(\rho_p - \rho_f)g}\frac{dp_S}{dz} \tag{13}$$

which shows the simple connection between p_S and ε_S.

Using the experimental axial pressure profile in the spout at minimum spouting in a bed of height H_m, ε_S was calculated from Eq. (13) and the results are shown in **Fig. 9** along with the profiles obtained using the different pressure profiles in the spout. The Lefroy and Davidson[5] and Grbavcic *et al.*[3] profiles in Fig. 9 are obtained by applying their spout pressure distributions in Eq. (13).

Morgan *et al.*[14] have calculated the spout voidage distribution at minimum spouting using a variational technique and boundary conditions $\varepsilon_S(0)=1$ and $\varepsilon_S(H)=\varepsilon_{mF}$. Their solution shows that there is no variational solution at minimum spouting for which ε_S decreases monotonically that can satisfy the aforementioned boundary conditions unless a particular parameter C_0 is bounded by 0.215 and 0.785. Since the values of C_0 are 0.78 for 0.574-mm particles and 0.71 for 0.964-mm particles at minimum spouting in a bed of height H_m, the axial voidage profiles for these cases are also shown in Fig. 9.

Although the voidage profiles calculated from Eq. (13) using the experimental spout pressure distribution are similar in shape to those from other methods, there are substantial differences in ε_S as z/H_m approaches zero. Since Morgan *et al.*[14] specified the boundary condition, $\varepsilon_S(0)=1$, and the slope of the axial spout pressure profiles of Lefroy and Davidson[5] and Grbavcic *et al.*[3] is zero at $z=0$, $\varepsilon_S(0)$ is one of these cases. This is not so, however, in our cases. As can be seen in Fig. 9, the spout voidage distributions calculated from Eq. (13) using the experimental spout pressure distributions are more uniform axially compared to the profiles reported for representing coarse particle beds. Note that $\varepsilon_S(0)<1$ and $\varepsilon_S(0)$ approach an asymptotic value of 1 as the particle size is increased.

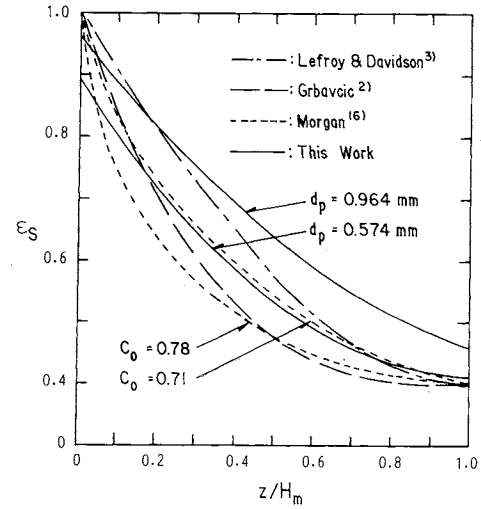

Fig. 9. Voidage profiles in the spout: $u = u_{mS}$; $H = H_m$.

For the small particles of this study, it is observed that the particles enter the spout primarily in the region close to the spout inlet, and particles are observed in the inlet to the spout in agreement with the predicted spout voidage profiles.

The spout diameter is not always uniform axially and is substantially wider than the average near the top of the bed when H is approximately equal to H_m at the minimum spouting condition, but it becomes more uniform in beds shallower than H_m. For a given bed height, the spout diameter becomes more uniform as the fluid velocity is increased above the minimum and the average diameter increases with the flow rate, approximately following McNab's[12] relationship

$$d_S/(d_S)_{mS} = (u/u_{mS})^{1/2} \tag{14}$$

for velocities up to $1.5u_{mS}$. Above this velocity, Eq. (14) overpredicts our data.

The spout pressure drop, ΔP_S, did not vary greatly with the inlet flow rate above the minimum, but the normalized axial pressure profile in the spout became flatter than that at minimum spouting as the inlet flow rate was increased above the minimum.

4. Conclusions

1. The fluid streamlines in the annulus are well represented by our model.

2. The average fluid velocity at the top of the annulus, calculated from the model, decreases as the particle size and bed height decrease.

3. The calculated fluid residence time in the annulus is broad and the calculated values are about 27% lower than those measured.

4. For the fine particle system studied, $\varepsilon_S(0)$ was less than one and the axial voidage calculated was more uniform than that for coarse particle systems.

Acknowledgement

One of the authors (S. J. Kim) gratefully acknowledges the support of this work by the Korea Science and Engineering Foundation.

Nomenclature

$$C_0 = \int_0^1 \frac{1-\varepsilon_S}{1-\varepsilon_{mF}} d(z/H) = \Delta P_{mS}/\Delta P_{mF} + \frac{\rho_f[(D_C/(d_S)_{mS})^4 u_{mS} - \varepsilon_{mF} u_{SH}^2]}{[(1-\varepsilon_{mF})(\rho_p-\rho_f)gH]} \quad [—]$$

d_i	=	spout inlet tube diameter	[mm]
d_p	=	particle diameter	[mm]
d_s	=	mean spout diameter	[mm]
D_S	=	d_S at $u=u_{mS}$ and $H=H_m$	[mm]
D_C	=	column diameter	[mm]
D_h	=	hydraulic diameter of the column	[mm]
f_1	=	$150[(1-\varepsilon)^2/\varepsilon^3][\mu/d_p^2]$	[—]
g	=	gravitational acceleration	[m/s^2]
h	=	H/H_m	[—]
H	=	bed height	[mm]
H_m	=	maximum spoutable height in the condition of minimum spouting	[mm]
H_p	=	jet penetration or spour fountain height	[mm]
I_0	=	modified Bessel Function (1st kind, order zero)	[—]
I_1	=	modified Bessel Function (1st kind, order one)	[—]
K_0	=	modified Bessel Function (2nd kind, order zero)	[—]
K_1	=	modified Bessel Function (2nd kind, order one)	[—]
m	=	$\pi/2H$	[mm^{-1}]
p	=	dynamic fluid pressure in the annulus	[kPa]
P_S	=	fluid pressure in the spout along axis of symmetry	[kPa]
P_{Si}	=	fluid pressure in the spout close to spout-annulus interface	[kPa]
ΔP_{mF}	=	minimum fluidization pressure drop	[kPa]
ΔP_{Si}	=	$p_{Si}(0)-p_{Si}(H)$	[kPa]
ΔP_{mS}	=	$p_S(0)-p_S(H)$ at $u=u_{mS}$	[kPa]
r	=	distance from vertical axis of symmetry of the column	[mm]
r_C	=	column radius	[mm]
r_S	=	spout radius	[mm]
t	=	fluid residence time in annulus	[s]
$\bar{u}$	=	velocity vector of annulus fluid	[mm/s]
u_a	=	superficial fluid velocity in the annulus	[mm/s]
$\langle u_a(z)\rangle$	=	$\left[2\int_{r_S}^{r_C} u_a(r,z)rdr\right] \Big/ [r_C^2-r_S^2]$	[mm/s]
$\langle u_a\rangle^{H}{}_{m}$	=	$\langle u_a\rangle$ at $H=H_m$	[mm/s]
u_{mF}	=	minimum fluidization velocity	[mm/s]
u_{mS}	=	minimum spouting velocity	[mm/s]
$(u_{mS})_{H_m}$	=	u_{mS} at $H=H_m$	[mm/s]
u_S	=	interstitial fluid velocity in the spout	[mm/s]
u_{SH}	=	u_S at $z=H$	[mm/s]
v_S	=	interstitial particle velocity in the spout	[mm/s]
$\langle V_a\rangle$	=	$\langle u_a\rangle(\pi D_C^2/8)$	[mm^3/s]
$\langle V_a\rangle_{H_m}$	=	$\langle V_a\rangle$ at $H=H_m$	[mm^3/s]
z	=	vertical height in the column from spout inlet	[mm]
ε	=	bed voidage	[—]
ε_{mF}	=	voidage at minimum fluidization condition	[—]
ε_S	=	spout voidage	[—]
ζ	=	z/H	[—]
μ	=	fluid viscosity	[kg/m·s]
υ	=	kinematic viscosity of fluid	[m^2/s]
ρ_f	=	fluid density	[kg/m^3]
ρ_p	=	particle density	[kg/m^3]
ψ	=	stream function	[mm^3/s]
ψ	=	$\psi(u_{mF}r_C^2)$	[—]

Literature Cited

1) Epstein, N., C. J. Lim and K. B. Mathur: *Can. J. Chem. Eng.*, **56**, 436 (1978).
2) Epstein, N. and N. Levine: "Fluidization," J. F. Davidson and D. L. Kearns (Eds.), Cambridge Univ. Press, England, p. 198 (1979).
3) Grbavcic, Z. B., D. V. Vukovic, F. K. Zdanski and H. Littman: *Can. J. Chem. Eng.*, **54**, 33 (1976).
4) Grbavcic, Z. B.: M. Sc. thesis, Belgrade Univ., Yugoslavia (1975).
5) Lefroy, G. A. and J. F. Davidson: *Trans. Instn. Chem. Engrs.*, **47**, T120 (1960).
6) Lim, C. J. and K. B. Mathur: *AIChE J.*, **22**, 674 (1976).
7) Littman, H., M. H. Morgan, D. V. Vukovic, F. K. Zdanski and Z. B. Grbavcic: *Can. J. Chem. Eng.*, **55**, 497 (1977).
8) Littman, H., M. H. Morgan, P. V. Narayanan, S. J. Kim, J. Y. Day and G. M. Lazarek: *Can. J. Chem. Eng.*, **63**, 188 (1985).
9) Mamuro, T. and H. Hattori: *J. Chem. Eng. Japan*, **1**, 1 (1968).
10) Mathur, K. B. and N. Epstein: "Spouted Beds," Academic Press, New York (1974).
11) Mathur, K. B. and P. E. Gishler: *AIChE J.*, **1**, 157 (1955).
12) McNab, G. S.: *Brit. Chem. and Proc. Technol.*, **17**, 532 (1972).
13) Morgan, M. H. and H. Littman: "Fluidization," J. R. Grace and J. M. Matsen (Eds.), Plenum Press, New York (1980).
14) Morgan, M. H., J. Y. Day and H. Littman: *Chem. Eng. Sci.*, **40**, 1367 (1985).
15) Piccinini, N., J. R. Grace and K. B. Mathur: *Chem. Eng. Sci.*, **34**, 1957 (1979).
16) Rovero, G., C. M. H. Brereton, N. Epstein, J. R. Grace, L. Casalegno and N. Piccinini: *Can. J. Chem. Eng.*, **61**, 289 (1983).
17) Thorey, B., J. B. Sauby, K. B. Mathur and G. L. Osberg: *Can. J. Chem. Eng.*, **37**, 184 (1959).